

662677
DP-1447

TIS FILE
RECORD COPY

EVALUATION OF NEUTRON CROSS SECTIONS FOR ^{244}Cm , ^{246}Cm , AND ^{248}Cm

R. W. BENJAMIN
F. J. McCROSSON
W. E. GETTYS



SAVANNAH RIVER LABORATORY
AIKEN, SOUTH CAROLINA 29801

PREPARED FOR THE U.S. ENERGY RESEARCH AND DEVELOPMENT ADMINISTRATION UNDER CONTRACT AT(07-2) 1

NOTICE

This report was prepared as an account of work sponsored by the United States Government. Neither the United States nor the United States Energy Research and Development Administration, nor any of their contractors, subcontractors, or their employees, makes any warranty, express or implied, or assumes any legal liability or responsibility for the accuracy, completeness or usefulness of any information, apparatus, product or process disclosed, or represents that its use would not infringe privately owned rights.

Printed in the United States of America

Available from

National Technical Information Service

U.S. Department of Commerce

5285 Port Royal Road

Springfield, Virginia 22161

Price: Printed Copy \$4.00; Microfiche \$3.00

662671

DP-1447

Distribution Category: UC-34c

EVALUATION OF NEUTRON CROSS SECTIONS FOR ^{244}Cm , ^{246}Cm , AND ^{248}Cm

by

R. W. Benjamin

F. J. McCrosson

W. E. Gettys *

Approved by

P. L. Roggenkamp, Research Manager
Reactor Physics Division

Publication Date: January 1977

*Present Address: Clemson University
Clemson, SC 29631

**E. I. DU PONT DE NEMOURS AND COMPANY
SAVANNAH RIVER LABORATORY
AIKEN, SOUTH CAROLINA 29801**

PREPARED FOR THE U. S. ENERGY RESEARCH AND DEVELOPMENT ADMINISTRATION UNDER CONTRACT AT(07-2)-1

ABSTRACT

Neutron cross section data for ^{244}Cm , ^{246}Cm , and ^{248}Cm have been evaluated and put into the ENDF/B format. For each isotope, the neutron energy region from 10^{-5} eV to 10 keV has been described entirely with resolved and unresolved resonance parameters based on the results of differential and integral cross section measurements and isotope production studies. The cross sections from 10 keV to 10 MeV were derived with nuclear model calculations. The evaluated cross section data have been tested with multigroup isotope production codes against the results of five independent reactor production experiments representing a wide range of spectral hardness. The test results show that these cross section sets make possible useful production forecasts in thermal and near-thermal spectra. The cross section data have not been tested in very hard spectra.

CONTENTS

Introduction	5
Sources of Experimental Data	6
Thermal and Resonance Region Cross Sections	8
^{244}Cm Resonance Region	15
^{246}Cm Resonance Region	16
^{248}Cm Resonance Region	16
Fast Cross Sections	17
Average Number of Neutrons per Fission	23
Angular Distributions of Secondary Neutrons (^{246}Cm and ^{248}Cm)	23
Energy Distributions of Secondary Neutrons (^{246}Cm and ^{248}Cm)	24
Cross Section Data Testing	24
References	29

LIST OF TABLES

1	Summary of Differential Data	7
2	Summary of Integral Thermal Data	7
3	Summary of Production Experiments	8
4	Resonance Parameters for ^{244}Cm	10
5	Resonance Parameters for ^{246}Cm	11
6	Resonance Parameters for ^{248}Cm	12
7	Comparison of Evaluations with Integral Measurements	15
8	Optical Model Parameters for ^{246}Cm and ^{248}Cm	18
9	Fast Neutron Cross Sections for ^{246}Cm	19
10	Fast Neutron Cross Sections for ^{248}Cm	20
11	Inelastic Scattering Cross Sections for ^{246}Cm	21
12	Inelastic Scattering Cross Sections for ^{248}Cm	22

LIST OF FIGURES

1	Californium Production Chain	5
2	Capture Cross Sections for ^{244}Cm , ^{246}Cm , and ^{248}Cm Below 10 eV	13
3	Capture Cross Sections for ^{244}Cm , ^{246}Cm , and ^{248}Cm Below 100 eV	14
4	Comparison of Calculated and Measured Concentrations of Curium Isotopes	27

INTRODUCTION

[illegible]

FIGURE 1 Californium Production Chain

The cross sections and resonance parameters for ^{244}Cm , ^{246}Cm , and ^{248}Cm have been selected by evaluating the results of differential and integral cross section measurements, nuclear model calculations, and reactor production experience. Cross section measurements, both differential and integral, have been relatively sparse for the three isotopes because of the limited quantities (typically less than a few milligrams) of sufficiently pure sample material available for measurement. Consequently, only the cross sections for ^{244}Cm had been evaluated previously for inclusion in ENDF/B.¹ New differential measurements²⁻⁵ for all three isotopes made possible the evaluations for ^{246}Cm and ^{248}Cm and the re-evaluation of ^{244}Cm ; the nuclear model calculations and reactor production experience served to extend and strengthen these evaluations. The evaluated neutron cross sections were put into the Evaluated Nuclear Data File Library B (ENDF/B) Format⁶ through a contract funded by the Electric Power Research Institute.⁷ The evaluations are available through the National Neutron Cross Section Center at Brookhaven National Laboratory, Upton, NY 11973.

SOURCES OF EXPERIMENTAL DATA

Four primary data sources were used in the initial evaluation of the curium cross sections: differential measurements, integral measurements, nuclear model calculations, and reactor production experience. The useful differential cross section measurements are summarized in Table 1. Three series of total cross section measurements have been made and analyzed: early fast chopper measurements by Coté et al.⁸ and Berreth et al.,² and more recent Linac measurements at the Oak Ridge National Laboratory ORELA facility.^{3,4} Nuclear detonation measurements by Moore and Keyworth⁵ provided fission data above 20 eV and limited neutron capture data for ^{244}Cm and ^{246}Cm . Recent Russian fast chopper total cross section measurements by Kalebin⁹ gave results similar to those of References 2-4 and 8; Kalebin's results were received too late to be included in the evaluations. The primary contribution of these differential cross section data was to provide the resonance structure and resonance parameters throughout the energy regions indicated in Table 1. The differential measurements of these three isotopes produced few useful results in the thermal region of the even-mass curium isotopes because of their very small capture and fission cross sections. The differential fission cross section measurements⁵ gave useful results from the resonance region to about 3 MeV.

The integral thermal measurements¹⁰⁻¹⁴ summarized in Table 2 gave the initial estimates of the thermal capture cross sections for the even-mass isotopes; the thermal fission cross sections are so small as to be inconsequential in reactor or fuel cycle applications. The small thermal capture cross sections make

precision measurement difficult because of the significant background radioactivity in the sample. These thermal cross sections, therefore, carry large standard deviations.

TABLE 1

Summary of Differential Data

<i>Reaction Cross Section</i>	<i>Neutron Source</i>	<i>Isotope</i>	<i>Maximum Enrichment, atom %</i>	<i>Energy Region for Resonance Parameters, eV</i>	<i>Reference</i>
Total	Chopper (ANL)	^{244}Cm	96.5	0-275	8
		^{246}Cm	21.5	0-20	8
Total	Chopper (MTR)	^{244}Cm	93.8	0-90	2
		^{246}Cm	3.94	0-20	2
Total	Linac (ORELA)	^{244}Cm	82.5	0-525	3
		^{246}Cm	3.11	0-160	4
		^{248}Cm	96.8	0-2400	4
Fission ^a	Nuclear Explosion (PHYSICS-8)	^{244}Cm	98.5	20-980	5
		^{246}Cm	94.7	20-400	5
		^{248}Cm	89.3	20-100	5

a. Limited capture data for ^{244}Cm and ^{246}Cm .

TABLE 2

Summary of Integral Thermal Data

<i>Isotope</i>	<i>Capture</i>			<i>Fission</i>		
	$\sigma_{n\gamma}^{2200}, b$	<i>Error, %</i>	<i>Reference</i>	σ_{nf}^{2200}, b	<i>Error, %</i>	<i>Reference</i>
^{244}Cm	14	±30	10	1.1	±45	11
				1.0	±20	12
^{246}Cm	1.5	±33	10	0.17	±60	11
	1.2	±33	13	0.14	±36	12
^{248}Cm	2.63	±10	14	0.34	±21	11
	3.0	±33	10	0.39	±18	12

The thermal cross sections can be further limited by iterating through the testing procedure and comparing the results with the reactor production experience of the Savannah River Plant (SRP).¹⁵ The exact approach will be described subsequently, but the production experiments are listed in Table 3. The experiments are designated by number and characterized by the ratio of the epithermal to the thermal neutron flux. For all of these experiments, the initial isotopic concentrations were measured, the neutron flux history was monitored, and the final isotopic concentrations were measured. The initial nuclide column indicates the major initial components.

TABLE 3

Summary of Production Experiments

<u>Experiment</u> <u>Identification</u> <u>Name</u>		<u>Fast/Slow</u> <u>Flux Ratio</u> ^a	<u>Initial</u> <u>Nuclide(s)</u>	<u>Integrated</u> <u>Thermal Flux,</u> <u>n/cm²</u>
1	HIFLUX	0.3	²⁴² Pu	$3.8-9 \times 10^{22}$
2	Q-FOILS	0.3	²⁴³ Am, ²⁴⁴ Cm	1×10^{23}
3	HOUSINGS	0.7	²⁴² Pu	1.2×10^{23}
4	BARELAT	1.9	²⁴⁴ Cm	1.8×10^{21}
5	HARDLAT	9.2	²⁴⁴ Cm	2.5×10^{20}

$$a. \text{ Fast/Slow Flux Ratio} \equiv \frac{\int_{0.624 \text{ eV}}^{10 \text{ MeV}} \phi(E) dE}{\int_0^{0.624 \text{ eV}} \phi(E) dE}$$

THERMAL AND RESONANCE REGION CROSS SECTIONS

Below 10 keV, the neutron cross sections for ²⁴⁴Cm, ²⁴⁶Cm, and ²⁴⁸Cm are described entirely by the Breit-Wigner, single-level formula using the bound level (²⁴⁴Cm only), resolved, and unresolved resonance parameters listed in Tables 4-6. The potential (hard sphere) scattering cross sections associated with the resonance parameters and listed in the tables were calculated at 10 keV with the spherical optical model calculations to be described later.

The capture cross sections in the thermal and resonance regions below 100 eV are shown for the three isotopes in Figures 2 and 3. Figure 2, a log-log plot, shows clearly the assumed $1/v$ cross section in the thermal region due almost entirely to tailing from the resolved resonances in each isotope. The resonance region on a semilog plot from 0 to 100 eV (Figure 3) shows the expected similarity of resonance size and location for the three curium isotopes. In this energy region, the only resonances that might be missing would be for ^{246}Cm in the region between 15 and 85 eV. Errors* in the evaluated thermal and low-energy resonance region are estimated to be 10% where differential, integral, and production studies were used. The estimated error then increases gradually to about 25% at 10 keV where the theoretical calculations describe the cross section. Errors of 10% in the low-energy region are consistent with compounding the errors in the differential experiments²⁻⁵ and careful examination of the best integral experiments in conjunction with the consistent set production studies.¹⁴ The 25% error in the capture cross section above 10 keV is based on experience with similar theoretical calculations for nuclides whose cross sections were measured.

Fission cross sections in the low-energy region were fabricated by assigning reasonable fission widths to the resonances below 20 eV where no differential fission data exist. The intention was to obtain reasonable approximations to the measured thermal fission cross sections and fission resonance integrals simultaneously,^{11,12} a criterion which could not be met. The thermal fission cross sections, though small, cannot be described by tailing from the resolved resonances and a bound level without assigning an excessively large fission width to the bound level. The evaluations are compared with measured integral values in Table 7. Because the fission cross sections for the even-mass isotopes represent typically only 5 to 10% of the absorption cross section in the thermal and low-energy region, the extensive effort required to match more precisely the measured integral fission data was not undertaken. Thus, the fission cross section errors in this region are large, typically around 80%. From 50 eV to 300 keV, reasonable fission data are available, and the error is about 30%. Above the fission threshold at 300 keV, counting statistics are much better, and the error drops to about 15%.

* Error is used to indicate the standard deviation.

TABLE 4

Resonance Parameters for ^{244}Cm

E_0 , eV	Γ_n , meV	Γ_γ , meV	Γ_f , meV	E_0 , eV	Γ_n , meV	Γ_γ , meV	Γ_f , meV
-1.48	0.0633	23	0.50	264.8	11.39	40	0.92
7.667	9.4	32	0.45	274.2	21.53	35	0.39
16.785	1.88	37	1.40	317.4	6.06	35	0.28
22.825	0.855	35	3.50	329.5	42.29	45	0.41
35.0	3.79	23	1.57	343.6	47.08	30	0.80
52.8	0.61	35	1.60	353.1	117.4	35	1.22
70.05	0.653	20	1.70	361.8	22.83	42	1.38
86.05	25.6	30	0.52	364.6	6.11	39	2.20
96.3	6.77	51	2.33	386.3	26.14	30	0.90
132.9	11.53	46	1.62	397.6	17.95	39	0.70
139.2	2.36	30	2.70	414.0	21.36	35	0.21
171.3	3.01	34	1.17	420.6	123.1	33	0.85
181.6	8.76	34	1.84	426.9	20.66	19	0.18
197.0	32.28	50	1.34	443.7	67.41	41	1.00
209.8	45.19	34	0.48	471.1	44.28	46	2.80
222.1	41.43	52	1.80	489.2	22.12	20	0.27
230.7	15.04	50	0.50	492.1	51.45	33	0.42
234.5	3.98	41	0.85	511.1	123.0	41	0.22
242.7	1.293	36	2.20	520.6	40.16	28	1.61

Potential Scattering Cross Section = 10.32 b

Unresolved Resonance Parameters ($525 \text{ eV} \leq E_n \leq 10 \text{ keV}$)

Orbital Angular Momentum (ℓ)	Statistical Spin Factor (g)	Average Level Spacing (\bar{D}), eV	$\overline{\Gamma_n^o}$, meV	$\overline{\Gamma_\gamma}$, meV	$\overline{\Gamma_f}$, meV
0	1	14.1	1.695	36.24	1.35
1	1	14.1	1.234	36.24	1.35
1	2	7.05	0.725	36.24	0.675

TABLE 5

Resonance Parameters for ^{246}Cm

E_0 , eV	Γ_n , meV	Γ_γ , meV	Γ_f , meV	E_0 , eV	Γ_n , meV	Γ_γ , meV	Γ_f , meV
4.315	0.332	31	1.67	250.7	9.34	37	0.38
15.33	0.548	31	0.48	278.3	7.01	37	1.30
84.62	26.7	31	0.70	288.2	59.4	37	0.31
91.91	15.9	37	0.17	313.4	24.8	37	1.50
158.7	28.9	37	0.73	381.1	117.1	37	1.80

Potential Scattering Cross Section = 10.47 b

Unresolved Resonance Parameters ($385 \text{ eV} \leq E_n \leq 10 \text{ keV}$)

Orbital Angular Momentum (l)	Statistical Spin Factor (g)	Average Level Spacing (\bar{D}), eV	$\overline{\Gamma_n^0}$, meV	$\overline{\Gamma_\gamma}$, meV	$\overline{\Gamma_f}$, meV
0	1	38	2.3	37	0.48
1	1	38	2.0	37	0
1	2	19	1.0	37	0

TABLE 6

Resonance Parameters for ^{248}Cm

E_0 , eV	Γ_n , meV	Γ_γ , meV	Γ_f , meV	E_0 , eV	Γ_n , meV	Γ_γ , meV	Γ_f , meV
7.247	1.67	23.3	1.40	958.6	108.4	26	8.2
26.9	19.6	32.0	0.08	994.2	123.0	26	8.2
35.01	11.7	30.2	2.40	1042	190.5	26	8.2
76.1	96.8	26.0	3.3	1103	219.2	26	8.2
98.95	149.2	26.0	4.7	1194	328.2	26	8.2
140.3	1.53	26.0	8.2	1210	34.8	26	8.2
186.4	4.25	26.0	8.2	1262	270.0	26	8.2
237.9	16.5	26.0	8.2	1277	178.6	26	8.2
258.7	62.7	26.0	8.2	1288	53.8	26	8.2
321.8	26.4	26.0	8.2	1389	406.2	26	8.2
380.6	93.6	26.0	8.2	1505	682.8	26	8.2
415.7	50.0	26.0	8.2	1646	129.8	26	8.2
457.7	75.5	26.0	8.2	1812	544.9	26	8.2
484.9	9.7	26.0	8.2	1910	118.0	26	8.2
541.8	384.1	26.0	8.2	2040	198.7	26	8.2
605.3	105.8	26.0	8.2	2071	782.7	26	8.2
647.0	109.4	26.0	8.2	2138	471.6	26	8.2
688.6	39.4	26.0	8.2	2156	157.9	26	8.2
694.3	202.9	26.0	8.2	2215	654.2	26	8.2
721.5	91.3	26.0	8.2	2234	85.1	26	8.2
769.4	61.0	26.0	8.2	2291	330.3	26	8.2
865.9	491.6	26.0	8.2	2369	496.5	26	8.2
887.1	98.3	26.0	8.2	2391	322.7	26	8.2

Potential Scattering Cross Section = 10.40 b

Unresolved Resonance Parameters ($2.4 \text{ keV} < E_n < 10 \text{ keV}$)

Orbital Angular Momentum (ℓ)	Statistical Spin Factor (g)	Average Level Spacing (\bar{D}), eV	$\overline{\Gamma_n}$, meV	$\overline{\Gamma_\gamma}$, meV	$\overline{\Gamma_f}$, meV
0	1	40	4.8	26	0.32
1	1	40	9.6	26	0.32
1	2	20	4.8	26	0.32

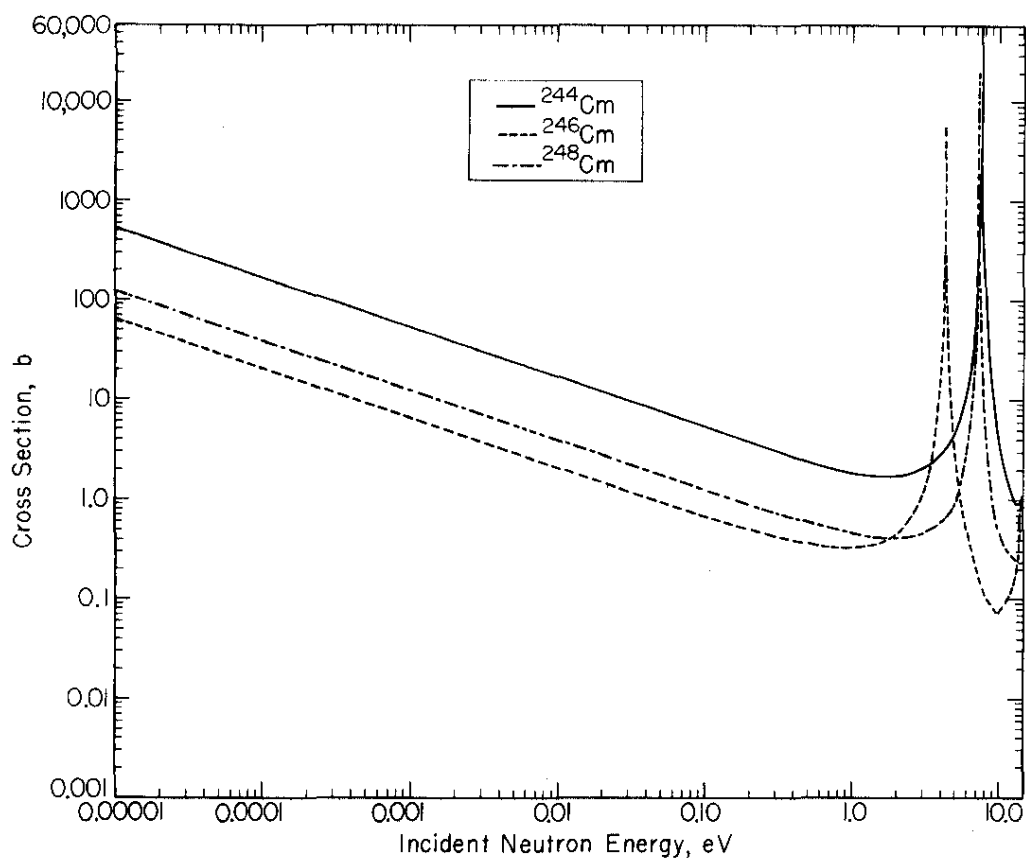


FIGURE 2 Capture Cross Sections for ^{244}Cm , ^{246}Cm , and ^{248}Cm Below 10 eV

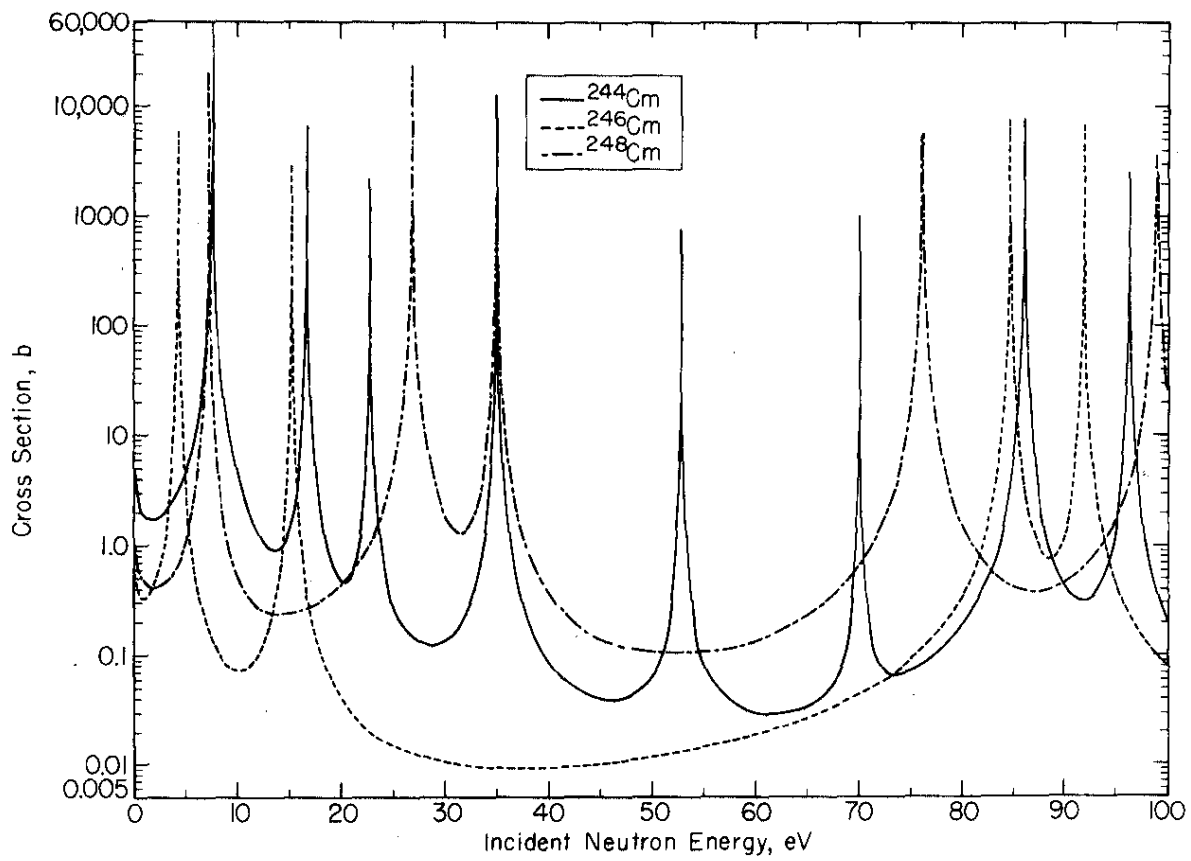


FIGURE 3 Capture Cross Sections for ^{244}Cm , ^{246}Cm , and ^{248}Cm Below 100 eV

TABLE 7

Comparison of Evaluations with Integral Measurements

Reaction	Isotope	σ (thermal), b		I (>0.5 eV), b		Reference
		Measured	Evaluated	Measured	Evaluated	
Capture	^{244}Cm	14 ± 4	10.4	650 ± 50	590	10
	^{246}Cm	1.5 ± 0.5	1.3	85 ± 15	104	10
		1.2 ± 0.4		121 ± 7		13
	^{248}Cm	2.63 ± 0.27	2.44	267 ± 27	246	14
		3.0 ± 1.0		275 ± 75		10
Fission	^{244}Cm	1.1 ± 0.5	0.6	18.0 ± 1.0	19.0	11
		1.0 ± 0.2		13.4 ± 1.5		12
	^{246}Cm	0.17 ± 0.1	0.06	10.0 ± 0.4	9.91	11
		0.14 ± 0.05		13.3 ± 1.5		12
	^{248}Cm	0.34 ± 0.07	0.12	13.2 ± 0.8	17.2	11
		0.39 ± 0.07		13.1 ± 1.5		12

 ^{244}Cm Resonance Region

Expansion of the bound and resolved resonance parameters for ^{244}Cm gives 2200 m/sec cross section values of:

$$\sigma_{n\gamma} = 10.4 \text{ b}$$

$$\sigma_{nf} = 0.6 \text{ b}$$

$$\sigma_{nn} = 7.2 \text{ b}$$

$$\sigma_{nT} = 18.2 \text{ b}$$

The total cross section above differs from the thermal value of the total cross section obtained experimentally by Berreth et al.² ($23 \pm 3 \text{ b}$); but this difference is not considered significant because their data were not corrected for small angle scattering from oxygen. Such a correction, for example, reduced the 2200 m/sec total cross section for ^{242}Pu from 39.1 to 26.96.¹⁶

The resonance parameters are primarily those determined by Simpson et al.¹⁷ through a simultaneous parametric fitting of the differential data in References 2, 3, and 5. Parameters of the bound and first-resolved resonance were modified within the quoted experimental uncertainty to obtain agreement with the integral data and production studies. The resonances are all s-wave resonances and they extend to 525 eV.

^{246}Cm Resonance Region

Parameters for 10 resolved s-wave resonances below 385 eV are based upon the results of References 2, 4, and 5. The parameters of the first resonance were modified within the experimental uncertainties to give reasonable agreement with the integral data and the production studies. A potential (hard sphere) scattering cross section of 10.466 b associated with these parameters was obtained from spherical optical model calculations described later. Expansion of the resonance parameters yields 2200 m/sec cross section values of:

$$\begin{aligned}\sigma_{n\gamma} &= 1.297 \text{ b} \\ \sigma_{nf} &= 0.063 \text{ b} \\ \sigma_{nn} &= 9.682 \text{ b} \\ \sigma_{nT} &= 11.042 \text{ b}\end{aligned}$$

The $\ell = 0$ unresolved resonances listed in Table 5 were derived from the PHYSICS-8 results.⁵ The $\ell = 1$ unresolved resonance parameters were selected such that the capture cross section from the combination of $\ell = 0$ and $\ell = 1$ parameters joins smoothly to the results of model calculations at 10 keV.

^{248}Cm Resonance Region

The resolved resonance region contains 46 resolved s-wave resonances and extends to 2.4 keV. The neutron and radiation widths are based on the ORELA total cross section measurements.⁴ Fission widths for the resonances at 26.9, 76.01, and 98.95 eV are based on the PHYSICS-8 measurements.⁵ All resonances above 100 eV have the same fission width $\bar{\Gamma}_f$. $\bar{\Gamma}_f$ was obtained by multiplying the average radiation width $\bar{\Gamma}_\gamma$ by the ratio of the PHYSICS-8 fission resonance integral² between 20 eV and 10 keV to the ORELA capture resonance integral⁴ between 20 eV and 10 keV. Expansion of the resonance parameters gives 2200 m/sec cross section values of:

$$\begin{aligned}\sigma_{n\gamma} &= 2.44 \text{ b} \\ \sigma_{nf} &= 0.117 \text{ b} \\ \sigma_{nn} &= 6.14 \text{ b} \\ \sigma_{nT} &= 8.70 \text{ b}\end{aligned}$$

The unresolved resonance region extends from 2.4 to 10 keV. The $\ell = 0$ unresolved resonance parameters are average parameters derived from the ORELA data.⁴ The $\ell = 1$ (p-wave) unresolved resonance parameters have a strength function based on an extrapolation of the curves of Lynn.¹⁸ An average fission width was chosen for both $\ell = 0$ and $\ell = 1$ unresolved resonances to give a smoother fission cross section across the interface at 10 keV.

FAST CROSS SECTIONS

Cross sections between 10 keV and 10 MeV were computed with nuclear model codes; only the fission cross sections have been measured. The fast cross sections for ^{244}Cm were taken from ENDF/B-IV, which contains the Dunford and Alter evaluation.¹ The fast cross sections in the Dunford and Alter work were fabricated through deformed optical model calculations.¹⁹ The COMNUC and CASCADE codes²⁰ provide a unified model for analyzing compound nuclear reactions.²¹ The calculated cross sections were joined to the lower energy cross sections at 10 keV.

Similar calculations were made at SRL for the fast cross sections of ^{246}Cm and ^{248}Cm . A spherical optical model²² was used to represent the two processes of direct or potential scattering of a neutron by the target and absorption of a neutron to form the compound nucleus. In the optical model, the neutron-target interaction is replaced by a complex single particle potential. The real part produces the average shape elastic scattering, and the imaginary part provides a mechanism for absorption or compound nucleus formation. In the present evaluation, the single particle potential is assumed to have the form

$$V(r) = -V_0 \cdot Y(a_1, r) - 4 \cdot W_0 \cdot i \cdot \frac{d}{dr} Y(a_2, r) - \frac{14 \text{ (MeV)}}{a_{1,r}} \cdot [j(j+1) - \ell(\ell+1) - 3/4] \frac{d}{dr} Y(a_1, r) \quad (1)$$

where

$$Y(a, r) = [1 + \exp(\frac{r-R}{a})]^{-1} \quad (2)$$

In Equation 1, ℓ is the orbital angular momentum of the incident neutron, and $j = |\ell \pm 1/2|$ is the total spin of the compound nucleus (the ground state spins of ^{246}Cm and ^{248}Cm are zero). The final term in Equation 1 accounts for spin-orbit interactions. Table 8 lists the values of the optical model parameters used in the calculations.

TABLE 8

Optical Model Parameters for ^{246}Cm and ^{248}Cm

<i>Parameter</i>	<i>Symbol</i>	<i>Value</i>
Real well depth	V_0	45 MeV
Imaginary well depth	W_0	10 MeV
Real well diffuseness	a_1	0.66 fermi
Imaginary well diffuseness	a_2	0.48 fermi
Well radius	R	$1.25A^{1/3}$ fermi
^{246}Cm		7.832 fermi
^{248}Cm		7.854 fermi

The optical model calculations were used primarily to determine the potential scattering cross section and transmission coefficients that serve to describe both formation and decay of the compound nucleus. The SRL versions of COMNUC and CASCADE were used to calculate the elastic, inelastic, capture, fission, and (n,2n) cross sections. The fission parameters were determined by varying them in the Hill-Wheeler²³ formalism until good fits to the fast fission cross section data of Moore and Keyworth⁵ were obtained. The computed cross sections are in Tables 9 and 10.

Cross sections for the excitation of discrete inelastic states and the inelastic continuum are given in Tables 11 and 12. Level energies for the first three levels in both ^{246}Cm and ^{248}Cm were taken from the compilation of Lederer et al.²⁴ Most of the remaining inelastic levels were inferred from similar, neighboring even-even nuclei. Level schemes for the odd-mass curium isotopes needed for (n,2n) calculations were obtained from Reference 25. Cross sections were determined for the excitation of discrete inelastic levels for incident neutron energies from 0.03 to 3.0 MeV. Between 0.5 and 3.0 MeV, the remaining (n,n') cross section was treated as a continuum of levels; above 3.0 MeV, the (n,n') reaction was treated wholly as a continuum. The codes on which these calculations are based yield an error of about 30%.

TABLE 9

Fast Neutron Cross Sections for ^{246}Cm

Energy, MeV	$\sigma_{n,n}, b$	σ_{α}, b	σ_f, b	$\sigma_{n,n'}, b$	$\sigma_{n,2n}, b$	$\bar{\nu}_L^*$
10.0	3.278	0	2.213	0.0084	0.3788	0.8801
9.0	3.593	0	2.289	0.0251	0.3084	0.8812
8.0	3.919	0	2.398	0.0876	0.1789	0.8863
7.5	4.145	0	2.427	0.1701	0.1005	0.8881
7.0	4.311	0	2.388	0.3220	0.0246	0.8900
6.5	4.480	0	2.216	0.5538	0	0.8876
6.0	4.646	0	1.952	0.8375		0.8852
5.0	4.842	0.0003	1.942	0.8309		0.8689
4.0	4.786	0.0015	1.874	0.8958		0.8426
3.0	4.316	0.0070	1.913	1.078		0.8012
2.5	3.912	0.0140	1.998	1.243		0.7663
2.0	3.478	0.0288	2.046	1.430		0.7168
1.5	3.330	0.0409	1.838	1.616		0.6407
1.2	3.660	0.0469	1.613	1.697		0.5855
1.0	4.070	0.0566	1.193	1.903		0.5413
0.7	5.934	0.0867	0.2493	1.832		0.4406
0.5	7.436	0.0895	0.0472	1.588		0.3565
0.3	9.132	0.0901	0.0057	1.366		0.2677
0.2	10.362	0.1023	0.0019	1.146		0.2094
0.1	11.885	0.1500	0.0006	0.8396		0.1250
0.07	12.498	0.1750	0.0005	0.6490		0.0918
0.05	13.076	0.2050	0.0005	0.3364		0.0670
0.03	13.618	0.2660	0	0		0.0412
0.02	13.702	0.3248				0.0276
0.01	13.624	0.4350				0.0275

* From the ^{244}Cm calculations.¹

TABLE 10

Fast Neutron Cross Sections for ^{248}Cm

Energy, MeV	$\sigma_{n,n}, b$	σ_{α}, b	σ_f, b	$\sigma_{n,n'}, b$	$\sigma_{n,2n}, b$	$\bar{\nu}_L^*$
10.0	3.327	0	2.500	0.01105	0.1044	0.8801
9.0	3.610	0	2.497	0.03208	0.1051	0.8812
8.0	3.969	0	2.466	0.1180	0.08684	0.8863
7.5	4.163	0	2.435	0.2040	0.06857	0.8881
7.0	4.355	0	2.321	0.3911	0.03377	0.8900
6.5	4.532	0	2.079	0.6989	0.00372	0.8876
6.0	4.679	0	1.254	1.548	0	0.8852
5.0	4.850	0.00005	1.253	1.527		0.8689
4.0	4.767	0.00031	1.230	1.538		0.8426
3.0	4.282	0.00166	1.304	1.680		0.8012
2.5	3.883	0.00370	1.431	1.810		0.7663
2.0	3.458	0.00951	1.629	1.883		0.7168
1.5	3.255	0.01917	1.897	1.728		0.6407
1.2	3.578	0.02865	1.999	1.472		0.5855
1.0	4.119	0.03447	2.023	1.589		0.5413
0.7	5.800	0.05783	1.004	1.521		0.4406
0.5	7.540	0.06699	0.2635	1.564		0.3565
0.3	9.357	0.06884	0.04386	1.439		0.2677
0.2	10.56	0.07722	0.01826	1.221		0.2049
0.1	12.08	0.1133	0.00891	0.9042		0.1250
0.07	12.71	0.1550	0.00778	0.6925		0.0918
0.05	13.36	0.2130	0.00756	0.3325		0.0670
0.03	13.98	0.3220	0.00746	0		0.0412
0.02	14.12	0.4190	0.00748	0		0.0276
0.01	14.18	0.6200	0.00787	0	0	0.00275

* From the ^{248}Cm calculations.¹

TABLE 11

Inelastic Scattering Cross Sections for ^{246}Cm

Energy, MeV	Level Energy, MeV											Continuum
	0.042	0.142	0.295	0.660	0.700	0.800	0.843	0.877	1.080	1.106	1.129	
3.00	0.0168	0.0144	0.0058	0.0078	0.0103	0.0053	0.0099	0.0098	0.0071	0.0091	0.0090	0.9727
2.50	0.0541	0.0439	0.0154	0.0221	0.0271	0.0115	0.0263	0.0250	0.0190	0.0233	0.0219	0.9534
2.00	0.1589	0.1187	0.0337	0.0591	0.0637	0.0205	0.0635	0.0561	0.0465	0.0521	0.0447	0.7125
1.50	0.3708	0.2360	0.0443	0.1418	0.1182	0.0225	0.1263	0.0941	0.0901	0.0843	0.0608	0.2268
1.20	0.5688	0.2977	0.0336	0.2262	0.1443	0.0124	0.1587	0.0979	0.0696	0.0462	0.0226	0.0190
1.00	0.8575	0.3714	0.0236	0.2925	0.1475	0.0045	0.1354	0.0628	0	0	0	0.0078
0.70	1.3505	0.3530	0.0053	0.1215	0	0	0	0				0.0017
0.50	1.423	0.1640	0.0010	0								
0.30	1.341	0.0250	0									
0.20	1.143	0.0030										
0.10	0.8396	0										
0.07	0.6490											
0.05	0.3364											
0.03	0											

TABLE 12

Inelastic Scattering Cross Sections for ^{248}Cm

Energy, MeV	Level Energy, MeV 0.043	0.144	0.300	0.660	0.700	0.800	0.843	0.877	0.950	1.010	1.080	1.106	1.129	Continuum
3.00	0.0047	0.0039	0.0015	0.0022	0.0029	0.0015	0.0028	0.0027	0.0012	0.0042	0.0020	0.0026	0.0025	1.6453
2.50	0.0170	0.0135	0.0046	0.0071	0.0085	0.0035	0.0084	0.0079	0.0141	0.0131	0.0061	0.0074	0.0069	1.7024
2.00	0.0602	0.0444	0.0123	0.0224	0.0239	0.0076	0.0241	0.0211	0.0127	0.0381	0.0178	0.0199	0.0169	1.5616
1.50	0.2099	0.1361	0.0261	0.0776	0.0648	0.0124	0.0692	0.0519	0.0397	0.1000	0.0491	0.0463	0.0340	0.8108
1.20	0.4159	0.2305	0.0272	0.1649	0.1114	0.0099	0.1180	0.0767	0.0554	0.0993	0.0499	0.0342	0.0181	0.0604
1.00	0.6866	0.2844	0.0163	0.2590	0.1354	0.0039	0.0071	0.0554	0.0234	0	0	0	0	0.0079
0.70	1.1315	0.2708	0.0034	0.1126	0	0	0	0	0	-	-	-	-	0.0026
0.50	1.4060	0.1572	0.0001	0	-	-	-	-	-	-	-	-	-	0.0007
0.30	1.4114	0.0275	0	-	-	-	-	-	-	-	-	-	-	0
0.20	1.2177	0.0028	-	-	-	-	-	-	-	-	-	-	-	-
0.10	0.9042	0	-	-	-	-	-	-	-	-	-	-	-	-
0.07	0.6925	-	-	-	-	-	-	-	-	-	-	-	-	-
0.05	0.3325	-	-	-	-	-	-	-	-	-	-	-	-	-
0.03	0	-	-	-	-	-	-	-	-	-	-	-	-	-

AVERAGE NUMBER OF NEUTRONS PER FISSION

The average number of neutrons per fission $\bar{\nu}(E)$ was based upon the work of Howerton.²⁶

$$\bar{\nu}(E) = \bar{\nu}_{th} + E[0.130 + 0.006(A-235)] \quad (3)$$

where E is the energy of the incident neutron in MeV, A is the atomic weight of the target nucleus in amu (i.e., 244, 246, or 248), and $\bar{\nu}_{th}$ is the thermal value for $\bar{\nu}(E)$. Because there have been no measurements of $\bar{\nu}_{th}$ for the even-mass isotopes, $\bar{\nu}_{th}$ was determined from the semiempirical formula of Gordeeva and Smirenkin²⁷ as modified by Manero and Konshin:²⁸

$$\nu_{th} = 0.2625Z + 0.0093A - 23.923 + \delta \quad (4)$$

where

$\delta = 0.09$ for odd-odd target nuclei

$\delta = 0$ for odd A -target nuclei

$\delta = -0.09$ for even-even target nuclei

Z = the atomic number

Equation 4 gives the following values for ν_{th} :

$$^{244}\text{Cm}: \bar{\nu}_{th} = 3.456 \text{ n/fission}$$

$$^{246}\text{Cm}: \bar{\nu}_{th} = 3.475 \text{ n/fission}$$

$$^{248}\text{Cm}: \bar{\nu}_{th} = 3.493 \text{ n/fission}$$

Gordeeva and Smirenkin²⁷ give a probable error of 3% in predictions of prompt $\bar{\nu}_{th}$ with an empirical approach; a more realistic evaluation is given by Manero and Konshin²⁸ who maintain that the present knowledge does not permit a prediction of this value to better than 10% for the transplutonium isotopes. The energy dependence of $\bar{\nu}(E)$ has an error of 1.5% in comparison of theory and experiment by Howerton;²⁶ thus, the overall error is dominated by the error in the thermal value and is about 10%.

ANGULAR DISTRIBUTIONS OF SECONDARY NEUTRONS (^{246}Cm and ^{248}Cm)

Angular distributions for elastically scattered neutrons are from the deformed nucleus optical model calculations of Dunford and Alter for ^{244}Cm .¹ They appear in the form of the cosine of the average scattering angle in the laboratory system μ_L . The values of μ_L are listed in Tables 9 and 10.

Angular distributions for (n,2n), (n,f), (n,n') to discrete levels, and (n,n') to the continuum are all assumed to be isotropic in the center-of-mass system since no experimental data exist.

ENERGY DISTRIBUTIONS OF SECONDARY NEUTRONS (^{246}Cm and ^{248}Cm)

Fission neutron energy distributions are assumed to conform to a simple Maxwellian fission spectrum with an effective nuclear temperature that obeys the expression:²⁸

$$T = 2/3 \{0.74 + 0.653 [\bar{v}(E) + 1]^{1/2}\} \quad (5)$$

Secondary neutron energy distributions for the inelastic continuum and the (n,2n) reactions are assumed to be evaporation spectra. The nuclear temperature for the inelastic continuum of ^{246}Cm and ^{248}Cm is described by the expression:^{29,30}

$$T(n,n') = \left(\frac{E'}{a}\right)^{1/2} \quad (6)$$

where

$$a = \frac{A}{10.433}$$

E' = secondary neutron energy, MeV

The expression for the temperature for the (n,2n) reaction in ^{246}Cm and ^{248}Cm is of the same general form:³⁰

$$T(n,2n) = \left(\frac{E'}{a+2}\right)^{1/2} \quad (7)$$

CROSS SECTION DATA TESTING

Data testing and data modifications have been done by using results of reactor production experiments with the SRL isotope depletion and production code GOSPEL. Since GOSPEL uses multi-group cross sections, the cross section evaluations were processed from the ENDF/B pointwise format into the SRL 84-group and 37-group representations. The energy groupings in these libraries are described in Reference 15.

GOSPEL uses a Runge-Kutta routine, stepping through time to solve the differential equations for isotopic transmutation. The loss for a given isotope is through decay (spontaneous fission, alpha, beta, or electron capture) or through neutron capture (n, γ to the ground state of the subsequent nucleus; n, γ to an isomeric state; or n,fission). The production of a given isotope is

determined by the losses of all the other isotopes that contribute to it through their decay or neutron interaction. The relative reaction rates of the nuclides are computed in GOSPEL by summing over the groups the product of the multigroup cross sections and computed multigroup flux spectra. The multigroup cross sections account for resonance self-shielding as a function of isotopic concentration by an equivalence principle. The multigroup flux spectra are computed by GLASS, which contains the lattice physics modules of the JOSHUA system. GLASS uses standard multigroup methods (typically in 37 or 84 energy groups) and treats spatial dependency by integral transport methods. Multiple flux spectra may be used in GOSPEL to account for spectral changes with time. Absolute thermal fluxes as a function of time must be specified separately. This specification is met by a combination of GLASS calculations and measurement of power produced in nearby fuel tubes. Time, rather than fluence, is thus the independent variable in the GOSPEL calculation.

In addition to cross sections for the even-mass curium isotopes, GOSPEL required suitable cross section data for the nuclides ^{242}Pu , ^{243}Am , ^{245}Cm , and ^{247}Cm . Older, existing ENDF/B evaluations for ^{242}Pu and ^{243}Am were brought up to date through the incorporation of recent resonance data;^{7,15} burnup of these two nuclides is well-described in GOSPEL with the improved evaluations. Evaluations were done for ^{245}Cm and ^{247}Cm with the relatively sparse experimental data available.^{7,15} The production calculations, however, are relatively insensitive to the cross sections of all four isotopes — ^{242}Pu , ^{243}Am , ^{245}Cm , and ^{247}Cm — within the range of the experimental uncertainties of the measured cross section data available for them. The even-mass curium isotopes are substantially more critical; small changes in the thermal capture cross sections of parameters of the first resonances may lead to significant changes in the burnup and production forecasts.

The production experiments have been described in considerable detail in Reference 15; a summary is given in Table 3. The fast-to-slow flux ratio is defined in terms of the total integrated flux in the fast and in the slow region. These experiments represent a cumulative total of 85 measurements of curium isotopic concentration after reactor irradiation in neutron spectra of varying hardness. Figure 4 shows the percent deviation of the calculated-to-measured concentration for these data points. The data are grouped roughly as to energy with the softer spectra measurements on top. Agreement of measurement and calculation within 20% for such high burnup would be acceptable; for these cases, however, 92% of the calculated concentrations fall within 10% of the measured concentrations, and all are within 15%. To achieve this quality of result, small adjustments were made to the thermal capture cross sections and the parameters of the

first resolved resonances; changes were within the quoted experimental error ($\sim 1 \sigma$). The integral cross sections from the experimental measurements and from the final evaluation are compared in Table 7. For ^{244}Cm , any significant increase in the thermal cross section, i.e., greater than a few tenths of a barn, completely destroys the good agreement between the calculated and measured isotopic concentrations.

These results represent reactor production forecasts in a wide variety of thermal and near-thermal spectra. The fast cross sections for these isotopes are reasonable extrapolations from theory and experiment, but have not been tested in very hard spectra. Thus, these cross sections can be used with confidence for thermal reactors and, with considerable caution, for fast reactors to predict heavy actinide concentrations as a function of time.

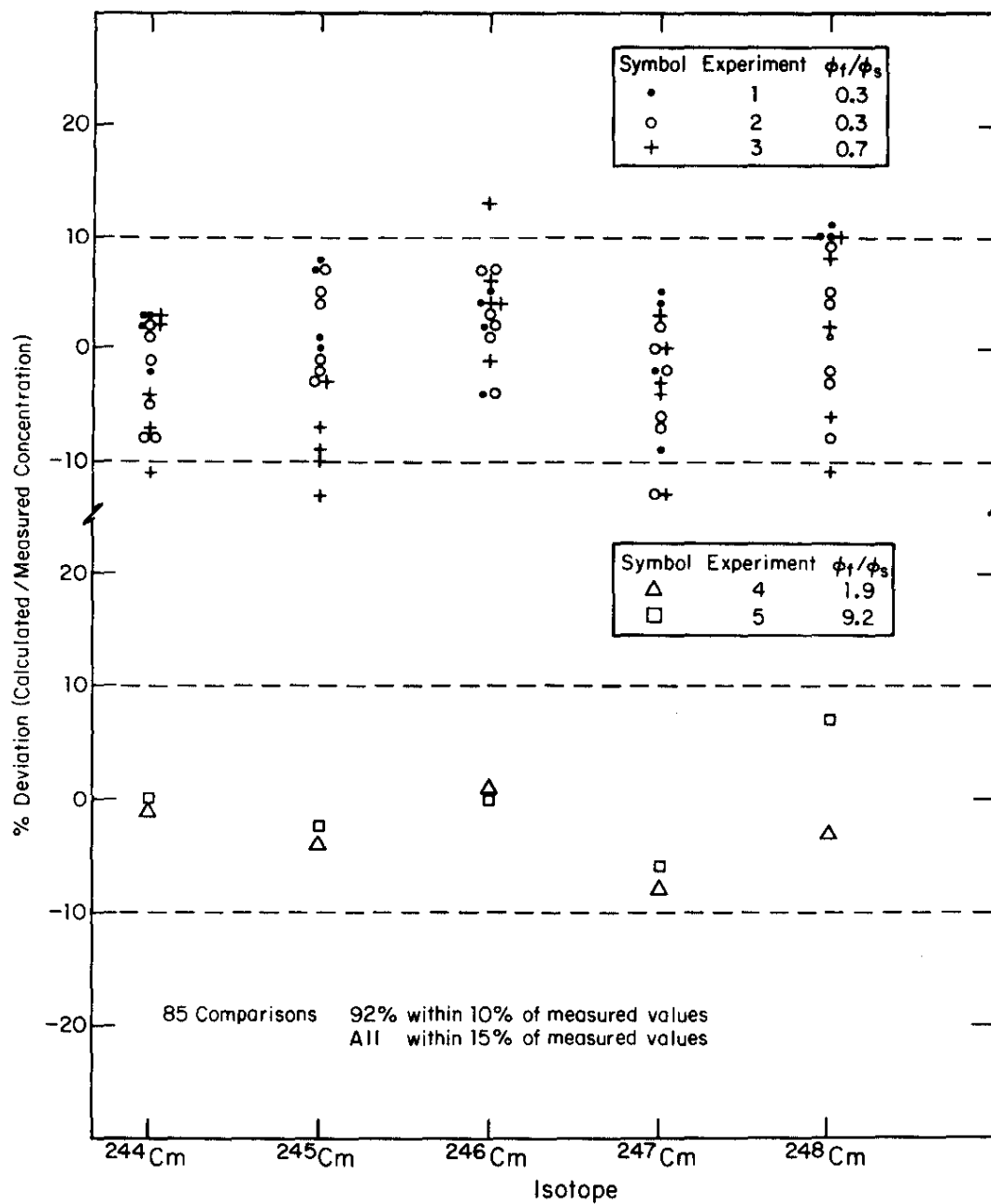


FIGURE 4 Comparison of Calculated and Measured Concentrations of Curium Isotopes

REFERENCES

1. C. L. Dunford and H. Alter. *Neutron Cross Sections for ^{238}Pu , ^{242}Pu , and ^{244}Cm* . USAEC Report NAA-SR-12271, Atomics International, Canoga Park, CA (1967).
2. J. R. Berreth, F. B. Simpson, and B. C. Rusche. "The Total Neutron Cross Sections of the Curium Isotopes from 0.01 to 30 eV." *Nucl. Sci. Eng.* 49, 145 (1972).
3. O. D. Simpson, F. B. Simpson, and T. E. Young (Idaho National Engineering Laboratory); J. A. Harvey and N. W. Hill (Oak Ridge National Laboratory); and R. W. Benjamin (Savannah River Laboratory) (personal communication).
4. R. W. Benjamin, C. E. Ahlfield, J. A. Harvey, and N. W. Hill. "Neutron Total Cross Section for Curium-248." *Nucl. Sci. Eng.* 55, 440 (1974).
5. M. S. Moore and G. A. Keyworth. "Analysis of the Fission and Capture Cross Sections of the Curium Isotopes." *Phys. Rev. C* 3, 1656 (1971).
6. D. Garber et al. (Editors). *ENDF-102, Data Formats and Procedures for the Evaluated Nuclear Data File*, ENDF. USERDA Report BNL-NCS-50496, Brookhaven National Laboratory, Nuclear Cross Section Center, Upton, NY (1975).
7. R. W. Benjamin, F. J. McCrosson, and P. L. Roggenkamp. *Conversion of ^{238}Pu and ^{252}Cf Production Chain Cross Section Data to ENDF/B-IV Format*. Report EPRI NP-161, Project 451, Electric Power Research Institute, Palo Alto, CA (1975).
8. R. E. Coté, R. F. Barnes, and H. Diamond. "Total Neutron Cross Section of ^{244}Cm ." *Phys. Rev.* 134, B1281 (1964).
9. S. M. Kalebin. "Total Neutron Cross Section Measurements on the Transactinium Isotopes ^{241}Am , ^{243}Am , ^{244}Cm , ^{245}Cm , ^{246}Cm , ^{248}Cm ." p 121 in *Transactinium Isotope Nuclear Data, Vol. II, Intern. At. En. Agency Publ., IAEA 186* (1976).
10. M. C. Thompson, M. L. Hyder, and R. J. Reuland. "Thermal Neutron Cross Sections and Resonance Integrals for ^{244}Cm through ^{248}Cm ." *J. Inorg. Nucl. Chem.* 33, 1553 (1971).
11. R. W. Benjamin, K. W. MacMurdo, and J. D. Spencer. "Fission Cross Sections for Five Isotopes of Curium and Californium-249." *Nucl. Sci. Eng.* 47, 203 (1972).

12. K. D. Zhuravlev and N. I. Kroshkin. "Thermal Neutron Fission Cross Sections and Fission Resonance Integrals of Curium Isotopes," Russian version in IAEA publication INDC(CCP)-68/G, *Nuclear Constants*, Vol. 19. Abstract in English in IAEA publication INDC(CCP)-70/U *Table of Content Translations of Soviet Reports Received by the INDC Secretariat* (1976).
13. J. Halperin, R. E. Druschel, and R. E. Eby. "Thermal Neutron Capture Cross Sections and Resonance Integral of ^{245}Cm and ^{246}Cm ." p 20 in *Chemistry Division Annual Progress Report for Period Ending May 20, 1969*. USAEC Report ORNL-4437, Oak Ridge National Laboratory, Oak Ridge, TN (1969).
14. R. E. Druschel, R. D. Baybarz, and J. Halperin. "The Thermal Neutron Capture Cross Section and Resonance Integral of ^{248}Cm ." p 23 in *Chemistry Division Annual Progress Report for Period Ending May 20, 1973*. USAEC Report ORNL-4891, Oak Ridge National Laboratory, Oak Ridge, TN (1973).
15. R. W. Benjamin, F. J. McCrosson, T. C. Gorrell, and V. D. Vandervelde. *A Consistent Set of Heavy Actinide Multigroup Cross Sections*. USERDA Report DP-1394, E. I. du Pont de Nemours and Company, Savannah River Laboratory, Aiken, SC (1975).
16. T. E. Young, F. B. Simpson, and R. E. Tate. "The Low-Energy Total Neutron Cross Section of Plutonium-242." *Nucl. Sci. Eng.* 43, 341 (1971).
17. O. D. Simpson, F. B. Simpson, and T. E. Young. "Evaluation of the ^{244}Cm Cross Sections in the Resonance Region." p 39 in *Nuclear Technology Division Annual Progress Report for Period Ending June 30, 1972*. USAEC Report ANCR-1088, Aerojet Nuclear Company, Idaho Falls, ID (1972).
18. J. E. Lynn. *The Theory of Neutron Resonance Reactions*. p 290, University Press, London, England (1968). (Note incorrectly labeled ordinate)
19. C. L. Dunford. *2-Plus, A Nonspherical Optical Model for Fast Neutron Cross Sections*. USAEC Report NAA-SR-11706, Atomics International, Canoga Park, CA (1966).
20. C. L. Dunford. *Compound Nucleus Reaction Analysis Programs COMNUC and CASCADE*. USAEC Report TI-707-130-013, Atomics International, Canoga Park, CA (1971).

21. C. L. Dunford. *A Unified Model for Analysis of Compound Nucleus Reactions*. USAEC Report AI-AEC-12931, Atomics International, Canoga Park, CA (1970).
22. H. E. Feshbach, C. E. Porter, and V. F. Weisskopf. "Model for Nuclear Reactions with Neutrons." *Phys. Rev.* 96, 448 (1954).
23. D. L. Hill and J. A. Wheeler. "Nuclear Constitution and the Interpretation of Fission Phenomena." *Phys. Rev.* 89, 1102 (1953).
24. C. M. Lederer, J. M. Hollander, and I. Perlman. *Tables of Isotopes*. Sixth Edition, John Wiley, New York (1968).
25. T. H. Braid, R. R. Chasman, J. R. Erskine, and A. M. Friedman. "(d,p) and (d,t) Studies of the Actinide Elements. II. ^{243}Cm , ^{245}Cm , ^{247}Cm , and ^{249}Cm ." *Phys. Rev.* 4C, 247 (1971).
26. R. J. Howerton. "Prediction of the Energy Dependence of the Average Yield of Neutrons per Fission of Isotopes of Thorium, Uranium, and Plutonium." *Nucl. Sci. Eng.* 46, 42 (1971).
27. L. D. Gordeeva and G. N. Smirenkin. "An Empirical Formula for the Average Number of Fission Neutrons." *Sov. At. En.* 14, 562 (1963).
28. F. Manero and V. A. Konshin. "Status of Energy Dependent $\bar{\nu}$ Values for the Heavy Isotopes (2790) from Thermal to 15 MeV and of $\bar{\nu}$ Values for Spontaneous Fission." *At. En. Rev.* 10, 637 (1972).
29. A. Foderaro. *The Elements of Neutron Interaction Theory*. MIT Press, Cambridge, MA, 408 (1971).
30. M. K. Drake and P. F. Nichols. *Neutron Cross Sections for ^{234}U and ^{236}U* . USAEC Report GA-8135, Gulf General Atomic Report, San Diego, CA (1967).